Polish Journal of Chemical Technology, 18, 3, 59—67, 10.1515/pjct-2016-0049

Catalytic activity of cobalt and cerium catalysts supported on calcium hydroxyapatite in ethanol steam reforming

Justyna Dobosz[1], Sylwia Hull[2], Mirosław Zawadzki[1*]

[1]Polish Academy of Sciences, Institute of Low Temperature and Structure Research, Department of Nanomaterials Chemistry and Catalysis, PO Box 1410, 50-950 Wroclaw, Poland
[2]Wroclaw University of Technology, Division of Chemistry and Technology Fuels, Gdanska 7/9, 50-344 Wrocław, Poland
[*]Corresponding author: e-mail: M.Zawadzki@int.pan.wroc.pl

In this paper, Co,Ce/$Ca_{10}(PO_4)_6(OH)_2$ catalysts with various cobalt loadings for steam reforming of ethanol (SRE) were prepared by microwave-assisted hydrothermal and sol-gel methods, and characterized by XRD, TEM, TPR-H_2, N_2 adsorption–desorption measurements and cyclohexanol (CHOL) decomposition tests. High ethanol conversion (close to 100%) was obtained for the catalysts prepared by both methods but these ones prepared under hydrothermal conditions (HAp-H) ensured higher hydrogen yield (3.49 mol H_2/mol C_2H_5OH) as well as higher amount of hydrogen formed (up to 70%) under reaction conditions. The superior performance of 5Co,10Ce/HAp–H catalyst is thought to be due to a combination of factors, including increased reducibility and oxygen mobility, higher density of basic sites on its surface, and improved textural properties. The results also show a significant effect of cobalt loading on catalysts efficiency in hydrogen production: the higher H_2 yield exhibit catalysts with lower cobalt content, regardless of the used synthesis method.

Keywords: hydroxyapatite, cobalt, cerium, ethanol steam reforming, hydrogen production.

INTRODUCTION

Nowadays, H_2 is mainly produced from fossil resources such as natural gas, LPG or gasoline, what is always associated with emissions of air pollutants[1]. Steam reforming of ethanol (SRE) is considered as one of alternative methods of hydrogen production. It is very attractive option because ethanol represents renewable resource (can be obtained from biomass fermentation without net addition of CO_2 to the atmosphere), is easier to store, safer to transport and considerable less toxic than other alcohols (e.g. methanol). Additionally, SRE requires significant less energy per mole of H_2 formed as compared to reforming of saturated hydrocarbons and produces mainly one byproduct (CO_2)[2].

So for, SRE has been investigated over a different noble (Rh, Pt, Ru, Pd, Ir)[3, 4] and base metals (Ni, Cu, Co, Ni–Co, Ni–Cu)[5–7] and over oxide catalysts such as MgO, Al_2O_3, ZnO, TiO_2, CeO_2, V_2O_5 or others[8, 9]. Noble based catalysts exhibit high catalytic activity over wide range of temperatures (400–600°C) in terms of hydrogen yield and ethanol conversion. However, the high price of these metals has paid attention to inexpensive alternative. Oxide catalysts show good activity but usually insufficient selectivity. Among base metal catalysts, Ni-based give high ethanol conversion with high selectivity to hydrogen but CH_4 or CO content in the reaction products is comparatively high[10]. Cu-based catalysts exhibit good activity but H_2 yield is relatively low[11]. Co-based catalysts provide comparable catalytic performance as the noble based catalysts and are characterized by a high C–C bond cleavage activity in the range of 300–500°C[12]. Most often Co-based catalysts are supported on various oxides like MgO, ZnO, Al_2O_3, SiO_2, ZrO_2, TiO_2, La_2O_3, Sm_2O_3 or CeO_2[13–15]. However, these catalytic systems are frequently deactivated during on-stream operation via coke formation, cobalt oxidation or sintering[16]. Therefore, in order to improve the performance of Co-based catalysts for SRE, a suitable support and convenient synthesis method should be selected.

Calcium hydroxyapatite (HAp), being a natural occurring mineral with the formula $Ca_{10}(PO_4)_6(OH)_2$, is the most studied compound of the apatite class. It crystallizes in the hexagonal structure in $P6_3/m$ space group and demonstrates a high chemical and thermal stability and a weak solubility[17–18]. Moreover, its very good ion–exchange ability causes that Ca^{2+} sites in the HAp structure can be easily substituted by various divalent, trivalent or quadrivalent ions what has a strong influence on surface characteristic (including acid-base properties), adsorptive activity, morphology and size of the particles[19]. Additionally, it has a mesoporous structure and can exhibit a high surface area and porosity, what makes it an interesting material for catalytic applications. The catalytic properties of HAp were reported in the oxidative dehydrogenation of propane[20] and decomposition of volatile organic compounds[21], as a catalysts support was investigated in such processes as glycerol steam reforming[22], oxidation of alcohols[23] or hydrogen generation from $NaBH_4$[24].

To our knowledge, HAp has not yet been used as a catalytic material for SRE. Thus, the aim of the present work was to assess the ability of cobalt and cerium promoted hydroxyapatites to convert ethanol into hydrogen via ethanol steam reforming. In our preliminary studies, we observed the deactivation of cobalt catalysts after a few hours on-stream due to carbon accumulation on their surface. Addition of ceria to Co-based catalyst should improve the catalytic performance and reduce the formation of coke species on the catalyst surface. CeO_2 has an oxygen storage property because of high oxygen mobility in its lattice, and therefore it may be a good choice for elevating resistance to coke formation. Furthermore, the effect of synthesis method of hyroxyapatite on catalysts activity in the SRE process was determined. The hydrothermal and sol-gel method of synthesis were used to prepare hydroxyapatites due to their simplicity and high crystallinity of products. These methods are also attractive as can produce nanosize HAp

under mild conditions. This study may provide the first evidence that Co,Ce/HAp are active system for SRE and show the effect of preparation method of calcium hydroxyapaties on catalysts activity and performance in ethanol steam reforming.

EXPERIMENTAL

HAp preparation

Microwave-assisted hydrothermal route

The appropriate amounts of $Ca(NO_3)_2 \cdot 4H_2O$ and $(NH_4)_2HPO_4$ (POCH, Poland) were dissolved in distilled water and then mixed together under vigorous stirring. The solution was adjusted to pH 10.5 by adding a 25% NH_3 solution. The hydrothermal treatment was conducted in microwave autoclave at 200°C for 1 hour. The resulting product was filtered and washed with distilled water and ethanol several times, dried at 80°C overnight and calcined at 500°C for 3 h under atmospheric conditions. Calcination temperature of 500°C was a little higher than reaction temperature to ensure the structural stability of hydroxyapatite during SRE conditions. The support synthesized by this method was denoted as HAp-H.

Sol-gel route

In this method, $Ca(NO_3)_2 \cdot 4H_2O$ and P_2O_5 (POCH) were used as precursors. First, the reagents were dissolved in 96% solution of ethanol (POCH) and then were mixed under vigorous stirring. The as-prepared solution was slowly transformed into a gel under continuously stirring at ambient temperature for 24 h. Subsequently, the formed gel was aged for 24 h and then was dried at 80°C in air for 24 h. Finally, the dried gel was calcined at 600°C for 3 h under atmospheric conditions. Calcination temperature of the sol-gel prepared support was higher than hydrothermal prepared support because precursors used for sol-gel synthesis generates a stable hydroxyapatite phase above 550°C[25]. The support prepared in this route was denoted as HAp-S.

Co,Ce/HAp preparation

Co,Ce/HAp catalysts with 5 or 7.5 wt% Co loading and 10 wt% Ce loading were prepared by incipient wetness co-impregnation method using an aqueous solution of cobalt $Co(NO_3)_2 \cdot 6H_2O$ (POCH) and cerium $Ce(NO_3)_3 \cdot 6H_2O$ (POCH) nitrates. After impregnation, the powders were dried overnight in air and then were calcined for 3 h at 500 or 600°C under atmospheric conditions for hydrothermal and sol-gel prepared support, respectively. The catalysts obtained on HAp-H support were denoted as Co,Ce/HAp-H, while the catalysts prepared on HAp-S support were denoted as Co,Ce/HAp-S.

Catalysts characterization

X-Ray diffraction (XRD) analysis was performed by X'Pert Pro (PANalytical Ltd.) diffractometer with a Ni-filtered CuKα radiation in the 2θ 10°–80° range. The analysis of XRD patterns was made using the FullProf Suite package for crystal structure solution and subsequent structure refinement. XRD data and Scherrer formula were used to average grain size calculations. The morphology of studied catalysts was characterized by transmission electron microscopy (TEM) using Philips CM-20 Super-Twin microscope operating at 200 kV with 0.25 nm resolution. To determine the surface chemical composition of the products the EDS (Energy Dispersive X-Ray Spectroscopy) analysis was employed. EDS measurements were performed using a FESEM FEI Nova NanoSEM 230 scanning electron microscopy equipped with EDS spectrometer (EDAX Genesis). The textural characteristics were achieved by conventional N_2 adsorption-desorption method at liquid nitrogen temperature, using Sorptomatic 1990 Instruments. Acid–base surface properties were determined by the analysis of results of cyclohexanol (CHOL) decomposition assuming that dehydration of CHOL to cyclohexene (CHEN) occurs over acid centers while dehydrogenation of CHOL to cyclohexanone (CHON) proceeds over both acid and base centers[26]. Therefore, the decomposition to CHEN is the measure of the surface's acid strength while CHON/CHEN selectivity ratio gives information about the basic nature of materials. Process was conducted in a continuous–flow fixed bed reactor at 300°C whereas the reaction products were analyzed by gas chromatograph equipped with FID detector. Susceptibility to hydrogen reduction was determined using AutoChem II 2920 analyzer. The temperature-programmed reduction (TPR) profiles were performed from room temperature to 1000°C with a step 5°C/min under an 5 vol% H_2 in Ar flow (50 ml/min).

Catalytic performance test

The catalytic tests were carried out in an electrically heated quartz tubular reactor (8 mm diameter) without the prior reduction of catalysts. About 200 mg of the catalyst with particle size between 0.45–0.75 tyler mesh was heated (2°C/min) in nitrogen stream (22 cm^3/min) up to 450°C. Prior to the introduction of a mixture of ethanol – water with a water to ethanol molar ratio of 6:1 into the reactor, the ethanol-water solution was vaporized into an evaporator. The gas hourly space velocity (GHSV) was 26 000 h^{-1}. The effluent products were analyzed on-line using a modified 504 M gas chromatograph equipped with FID and TCD detectors, and two packed columns filling Porapak Q and type S of active carbon.

The ethanol conversion was calculated using the following formula:

$$C = (C_2H_5OH_{in} - C_2H_5OH_{out})/C_2H_5OH_{in} \cdot 100\% \quad (1)$$

where $C_2H_5OH_{in}$ – inlet ethanol, $C_2H_5OH_{out}$ – outlet ethanol

whereas the hydrogen yield was calculated per mole of the inlet ethanol.

RESULTS AND DISCUSSION

Physicochemical properties

The XRD patterns of studied catalysts prepared by different methods are given in Figure 1. Diffractograms of both supports (Fig. 1A and B, pattern c) contain a sharp peaks assigned to the hexagonal hydroxyapatite phase crystallized in $P6_3/m$ space group (PDF No. 24-0333). Co- and Ce-containing samples also show well-formed hydroxyapatite structure and introduction of these ions don`t cause significant changes in intensity and width

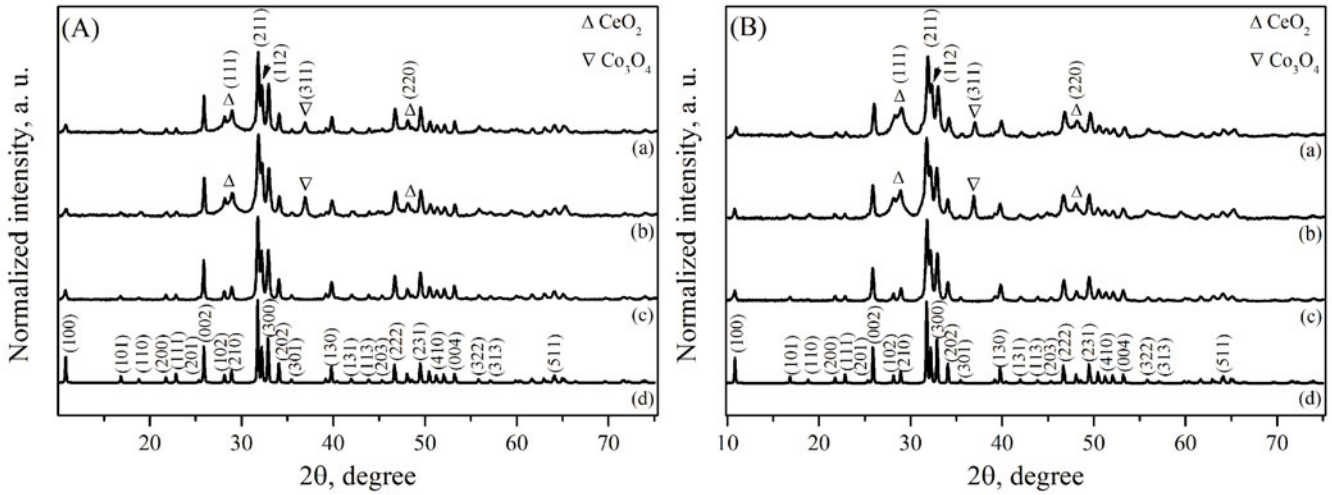

Figure 1. XRD patterns of hydroxyapatite catalysts (a) 5Co,10Ce/HAp, (b) 7,5Co,10Ce/HAp and (c) HAp prepared by (A) hydrothermal and (B) sol-gel method. Standard diffraction pattern of HAp (PDF No. 24-0333) is also presented as (d)

of the support peaks. However, XRD patterns of these materials show the additional reflections which come from cobalt and cerium oxides. The peaks at 2θ = 28.78° and 47.49° were assigned to cerium dioxide structure (PDF No. 02-1306), whereas the peak at 2θ = 28.78° was identificated as cobalt spinel phase Co_3O_4 (PDF No. 01-1152). The crystallite size of HAp supports was determined based on the position of peak at 2θ = 25.97° and 32.86° corresponding to (002) and (300) crystal planes, respectively. The average size of HAp-H crystallite is 30 nm while HAp-S samples are characterized by a smaller average crystallite size of about 17 nm. The average size of cobalt oxide crystallites was about 21 nm for Co,Ce/HAp-H and Co,Ce/HAp-S materials and did not change with increasing content of cobalt from 5 to 7.5 wt%.

The comparison of XRD patterns before and after ethanol steam reforming test for the 7.5Co,10Ce/HAp-H catalyst is shown in Figure 2. It is clearly seen that the intensity of Co_3O_4 peaks decreases under conditions of the SRE test and peaks assigned to CoO phase appear what can be evidently seen from the *inset* to Figure 2. Moreover, the XRD pattern of the used catalyst (Fig. 2b) contains other additional peaks, which correspond to metallic Co. It seems therefore that Co_3O_4 is partly reduced to CoO and Co phase during the catalytic test.

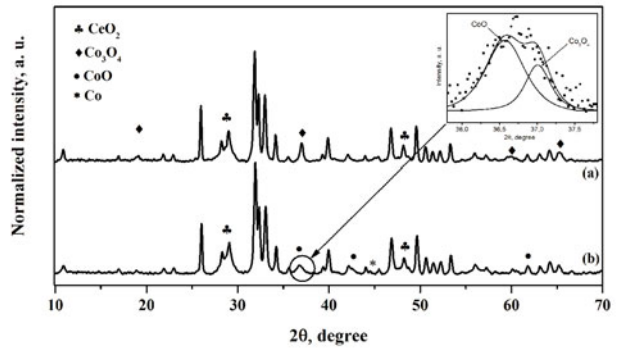

Figure 2. XRD patterns of 7,5Co,10Ce/HAp-H (a) before and (b) after steam reforming of ethanol reaction. *Inset* shows the 2θ region at ~ 37° characteristic of cobalt oxides

The morphology of both supports and Co,Ce/HAp catalysts was analysed by TEM and typical images are shown in Figure 3. HAp-H support is characterized by the isolated rod-like particles with an average length of 87 nm and average width of 28 nm (Fig. 3a). HAp-S support (Fig. 3b) exhibit however a more oval shape of particles with the high tendency to agglomeration. The average particle size of HAp-S is more difficult to calculate since TEM images contain both small and large, probably agglomerated, particles but it seems to be about 32 nm. TEM images of 5Co,10Ce/HAp samples are presented in Fig. 3c–d where small aggregated particles of size below 6 nm and larger with diameter of about 20 nm can be observed on the surface of the hydroxyapatite particles. Based on HRTEM images (not shown), smaller particles were identified as CeO_2 and larger as Co_3O_4 particles, respectively. The particle size of CeO_2 and Co_3O_4 in the catalyst samples containing 7.5 wt%Co was similar to that with 5 wt%Co.

Chemical composition of prepared samples was analysed by the EDS measurements. As shown in Table 1, the cobalt and cerium contents were in good agreement with expected ones for Co,Ce/HAp-H catalysts. For the Co,Ce/HAp-S samples, results of EDS analysis showed that the cobalt and cerium contents were a slight lover than nominal contents.

The textural properties of the studied materials were determined based on the N_2 adsorption-desorption isotherms and results are listed in Table 1. All samples displayed type IV isotherms (according to IUPAC classification) with a hysteresis loop characteristic for mesoporous materials. The most of pore sizes are distributed at the range 15–30 nm and 2–15 nm for HAp-H and HAp-S samples, respectively. It can be noticed from Table 1 that HAp-H samples ensure high specific surface area S_{BET} and the total pore volume V_{total} and the total pore area S_{total}, while HAp-S samples are characterized by significantly less advantageous textural properties. The observed decrease of V_{total} (by about 35%) as well as S_{total} and pore diameter D in the Co,Ce/HAp-H samples indicates that metal oxide particles are mainly incorporated inside the pores rather than on the external surfaces of

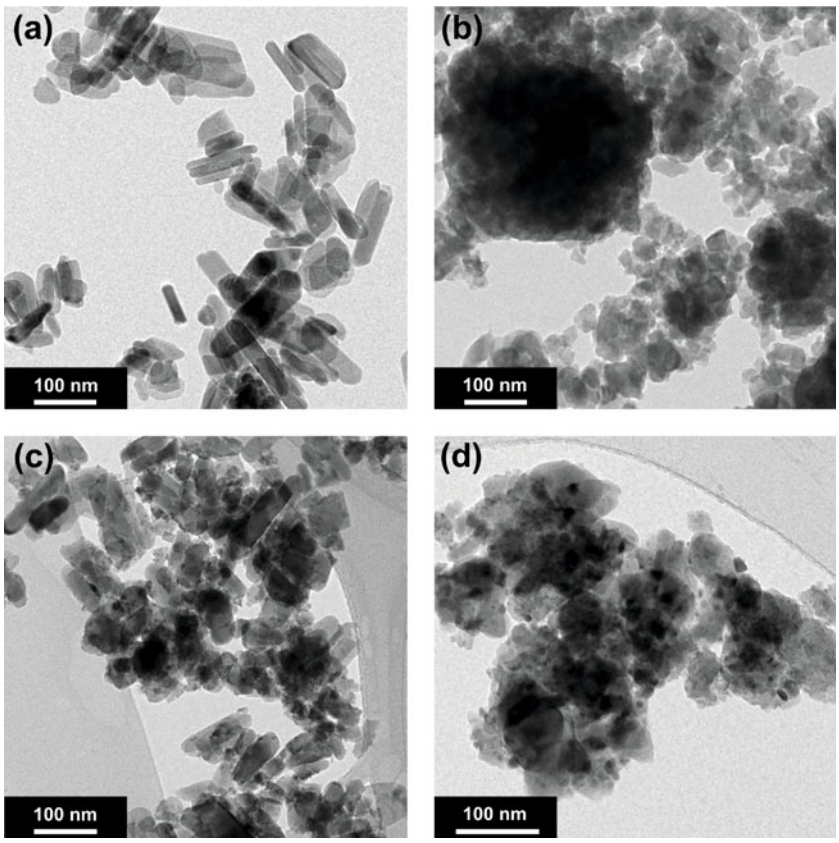

Figure 3. TEM images of (a) HAp-H, (b) HAp-S, (c) 5Co,10Ce/HAp-H and (d) 5Co,10Ce/HAp-S catalysts

Table 1. Specific surface area, pore volume and results of cyclohexanol decomposition

Sample	Chemical composition*		S_{BET} [m^2/g]	V_{total} [cm^3/g]	S_{Total} [m^2/g]	D [nm]	Conversion of CHOL[a] [%]	Selectivity to CHEN[b] [%]	Selectivity to CHON[c] [%]	Y[d]
	Co, wt%	Ce, wt%								
HAp – H	–	–	53.1	0.34	60.1	26	12.0	58.6	41.4	0.71
5Co, 10Ce/HAp – H	5.09	10.04	42.2	0.20	41.5	22	8.6	44.3	55.7	1.26
7.5Co, 10Ce/HAp – H	7.52	10.35	56.0	0.22	57.0	16	11.7	26.0	74.0	2.85
HAp – S	–	–	21.6	0.12	27.8	3.9	11.7	55.1	44.9	0.81
5Co, 10Ce/HAp – S	4.46	9.47	23.1	0.10	26.2	4.0	17.0	52.1	47.9	0.92
7.5Co, 10Ce/HAp – S	7.09	9.49	22.8	0.09	26.0	3.7	17.5	36.8	63.2	1.72

*Average content calculatated from EDS measurements, S_{BET} – specific surface area, S_{Total} – total pore area, D – maximum pore diameter.
[a] Cyclohexanol, [b] Cyclohexene, [c] Cyclohexanone, [d] CHOL/CHEN selectivity ratio.

the supports. It may suggest that some pores could be closed by the active ions what also should reduce the surface area. However, the presence of metal oxides on the HAp surface may affect S_{BET}. Opposite, only small textural changes in the S_{BET}, V_{total}, S_{total} or D are observed for the HAp-S supported catalysts.

In order to determine the acid–base properties of HAp and Co,Ce/HAp samples, the reaction of CHOL decomposition was used. As can be seen from Table 1, the HAp support prepared by both methods are characterized by the high selectivity toward dehydration of CHOL to CHEN what suggest that acid sites are mainly presented on the surface of these materials. Different behaviors in CHOL decomposition tests show Co, Ce containing catalysts. Namely, CHOL decomposition on the Co,Ce/HAp-H samples leads to the dehydrogenation of CHOL to CHON which is favored both by acid and basic sites. The high value of CHOL/CHEN selectivity ratio (Y) for these samples suggests the more basic nature of their surface. For the Co,Ce/HAp-S catalysts, the value of Y only slightly increases in comparison to the bare HAp-S support indicating the less predominance of basic sites on their surface.

Results of the TPR-H_2 measurements are presented in Fig. 4 and Table 2. According to the literature data[21], the reduction of Co_3O_4 proceeds in two steps: first, Co_3O_4

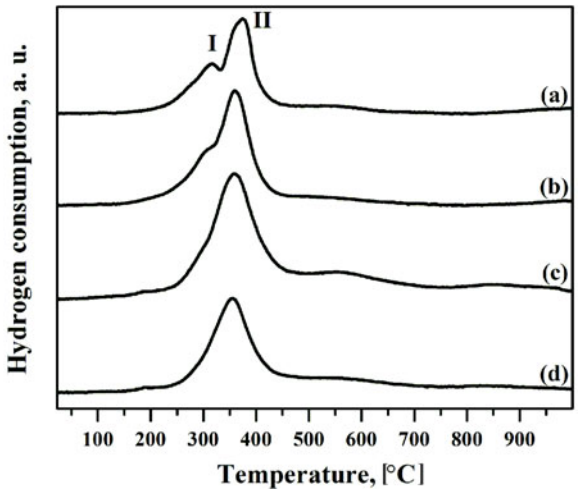

Figure 4. TPR-H_2 profile of (a) 5Co,10Ce/HAp-H, (b) 7,5Co,10Ce/HAp-H, (c) 5Co,10Ce/HAp-S, (d) 7,5Co,10Ce/HAp-S

Table 2. TPR-H_2 results of Co,Ce/HAp catalysts

Sample	Peak temperature, [°C]		H_2 consumption, [mol/g] · 10^3		Ratio (II)/(I)	Total consumption, [mol/g] · 10^3	
	(I)	(II)	(I)	(II)		Actual[a]	Theoretical[b]
5Co, 10Ce/HAp – H	314	373	0.382	1.013	2.65	1.395	1.152
7.5Co, 10Ce/HAp – H	312	361	0.582	1.466	2.52	2.048	1.701
5Co, 10Ce/HAp – S	–	358	–	1.028	–	1.028	1.009
7.5Co, 10Ce/HAp – S	–	354	–	1.736	–	1.736	1.604

[a] Estimated by quantification of H_2 uptake in TPR experiments.
[b] Amount of H_2 required for the complete reduction of Co_3O_4 to metallic Co.

is reduced to CoO ($Co_3O_4 + H_2 \rightarrow 3CoO + H_2O$) and then to the metallic cobalt ($CoO + H_2 \rightarrow Co + H_2O$). The TPR profile can contain one peak for each step and the intensity the first one to the second one should be 1:3. Some literature data reveal however that one broad reduction peak can also be observed[27]. In the case of CeO_2, literature data show that the TPR profiles also displays two reduction peaks. A low temperature peak (below 500°C) ascribed to the reduction of surface ceria and a high temperature peak (above 800°C) typical to the reduction of bulk ceria[28]. For the Co_3O_4–CeO_2 mixed oxide catalyst, the lack of the high reduction peak in the TPR profile was explained by the fact that cobalt is able to enhance the ceria bulk reducibility[29].

In our study, the TPR profiles of Co,Ce/HAp-H samples contain two peaks of H_2 consumption at about 310°C and around 365°C, corresponding to the Co_3O_4 reduction to CoO and next CoO to Co, respectively (Fig. 4a, b). The ratio of H_2 consumed in the second peak to that in the first peak is close to 3. For the Co,Ce/HAp-S catalysts, one broad peak centered at around 355°C with shoulder at lower temperature (Fig. 4c) is observed. This peak is also ascribed to the reduction of the Co_3O_4 oxide ($Co_3O_4 \rightarrow CoO \rightarrow Co$). However, on the basis of the TPR results obtained for both types of the Co,Ce/HAp catalysts one can not exclude the possibility of ceria reduction along with reduction of CoO to Co. As can be seen from Table 2, the H_2 amount required for the reduction of these samples is always higher compared to the theoretical values required for the complete reduction of Co_3O_4 to Co. This "extra H_2" can be related both to the ceria partial reduction and to the H_2 spillover to the support material. Therefore, it is very possible that reduction of cobalt species promotes reduction of dispersed ceria species. Over tested range of temperature, the reduction of HAp supports is almost not observed (TPR profiles are not shown).

Catalytic activity

Catalytic performance of hydroxyapatites was examined for the hydrogen production in the ethanol steam reforming process. First, the catalytic behavior of samples non-promoted by Co and Ce was evaluated. Results presented in Table 3 show that bare hydroxyapatites are nearly not active catalysts in the steam reforming of ethanol. The ethanol conversion at level of 8 and 24% in the last hour of SRE for the HAp-H and HAp-S supports are observed, respectively. For both support samples, the hydrogen yield was less than 1 mol H_2/mol C_2H_5OH during the whole process. The amount of hydrogen was around 6% after six hour of the test, whereas the high amount of carbon monoxide (CO) and aldehyde (CH_3CHO) was observed. Absence of carbon dioxide among reaction products proves that the reaction of ethanol steam reforming (reaction 2) does not occur over the used support materials:

$$C_2H_5OH + 3H_2O \rightarrow 2CO_2 + 6H_2 \quad (2)$$

Therefore, we expected that promotion with cobalt and cerium ions improved their catalytic performance. Results of the catalytic tests over Co,Ce/HAp-H and Co,Ce/HAp-S are shown in Table 3 and Fig. 5 and 6. As can be seen from Table 3, the 5Co,10Ce/HAp-H catalyst is characterized by the highest hydrogen yield (3.49 mol H_2/mol C_2H_5OH) over the entire time evaluated. During the SRE process such products as: H_2, CO_2, CO, CH_4, C_2H_4, CH_3CHO and CH_3COCH_3 were formed. The main product over this catalyst is hydrogen, however the large amount of CO is also formed (32%, Table 3) suggesting the incomplete ethanol steam reforming reaction (reaction 3). Further, the carbon monoxide may react with the steam and as the result the carbon dioxide may be obtained (reaction 4).

$$C_2H_5OH + H_2O \rightarrow 2CO + 4H_2 \quad (3)$$

$$CO + H_2O \rightarrow CO_2 + H_2 \quad (4)$$

The carbon monoxide can also take part in the catalytic methanation (reaction 5) decreasing the amount of H_2 in reaction product:

$$CO + 3H_2 \leftrightarrow CH_4 + H_2O \quad (5)$$

The small amount of methane may be also produced in ethanol decomposition to methane, hydrogen and carbon monoxide (reaction 6)

$$C_2H_5OH \rightarrow CH_4 + CO + H_2 \quad (6)$$

Table 3. Results of catalytic tests over hydroxyapatite catalysts after 6h of reaction at 450°C

Sample	C [%]	Y_{H2}, mol H_2/mol C_2H_5OH	Product distribution [%]						
			H_2	CO_2	CO	CH_4	CH_2CH_2	CH_3CHO	CH_3COCH_3
HAp – H	8.23	0.65	5.94	–	33.12	–	0.10	47.54	12.40
5Co, 10Ce/HAp – H	65.25	3.49	59.05	4.86	31.73	0.95	0.18	2.98	0.25
7.5Co, 10Ce/HAp – H	100.00	1.46	69.72	7.69	14.51	1.6	0.26	–	6.22
HAp – S	23.98	0.06	6.42	–	41.2	–	25.23	21.69	5.46
5Co, 10Ce/HAp – S	99.47	0.98	24.59	1.01	12.67	0.53	1.14	1.75	58.31
7.5Co, 10Ce/HAp – S	58.25	0.36	17.48	–	14.14	–	4.92	7.29	56.17

* C – Ethanol conversion, Y_{H2} – Hydrogen yield.

Over this catalyst, ethanol dehydrogenation to acetaldehyde (reaction 7), ethanol dehydration to ethylene (reaction 8) and ethanol decomposition into acetone (reaction 9) are taken place, too.

$$C_2H_5OH \rightarrow CH_3CHO + H_2 \quad (7)$$

$$C_2H_5OH \leftrightarrow CH_2CH_2 + H_2O \quad (8)$$

$$2C_2H_5OH \rightarrow CH_3COCH_3 + CO + 3H_2 \quad (9)$$

As can be seen, the steam reforming of ethanol over Co,Ce/HAp catalysts is very complex process in which many simultaneous and consecutive reactions can be involved what is in accordance with literature data[30].

The highest activity in SRE process, among studied catalysts, was obtained over the 7.5Co,10Ce/HAp-H catalyst. After 6 h of the reaction, this catalyst ensures the total ethanol conversion (Fig. 5a). The main reaction product is also hydrogen (70%; Fig. 6), which is mainly formed in the reaction of ethanol steam reforming (reaction 2), but the presence of CH_4 and CO in the reaction effluent suggests occurring the reaction of ethanol decomposition (reaction 6) and the incomplete ethanol steam reforming reaction (reaction 3).

Results of SRE process show that share of the carbon monoxide is lower over 7.5Co,10Ce/HAp-H than over 5Co,10Ce/HAp-H catalyst. Such result is in accord with that reported by Batista et al.[31] who found that the content of cobalt in the cobalt-based catalysts have influence on the amount of the carbon monoxide in the reaction products. Share of the CO in the post-reaction effluent also decreased with increasing the Co loading. Similarly, as for the 5Co,10Ce/HAp-H catalyst, the reactions of ethanol decomposition into acetone (reaction 9) and ethanol dehydration to ethylene (reaction 8) also occurred over 7.5Co,10Ce/HAp-H catalyst.

Hydroxyapatite supports prepared by the sol-gel method and impregnated with cobalt and cerium ions are able to transform the SRE precursors with almost complete ethanol conversion (99.5%; Table 3, Fig. 5). However, these catalysts ensure a quite small hydrogen yield (less than 1 mol H_2 per mol C_2H_5OH). The main reaction product over these catalysts is acetone, whereas share of H_2 in the reaction products is less than 25% and 20% for the 5Co,10Ce/HAp-S and 7.5Co,10Ce/HAp-S catalysts, respectively (Table 3). The acetone can be formed in such reaction as ethanol decomposition (reaction 9) or aldol condensation (reaction 10):

$$2CH_3CHO + H_2O \rightarrow CH_3COCH_3 + CO_2 + 2H_2 \quad (10)$$

Share of CO_2 in reaction products suggests that the SRE reaction does not occur over these catalysts. Small amount of CO_2 obtained over 5Co,10Ce/HAp-S catalyst

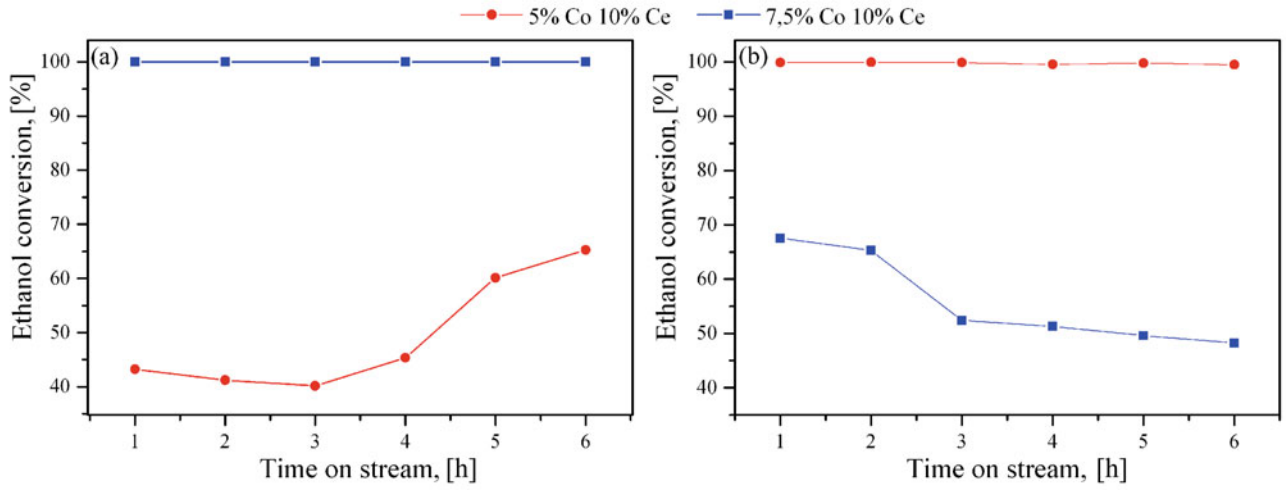

Figure 5. Ethanol conversion as a function of reaction time over catalysts prepared by (a) hydrothermal and (b) sol-gel methods

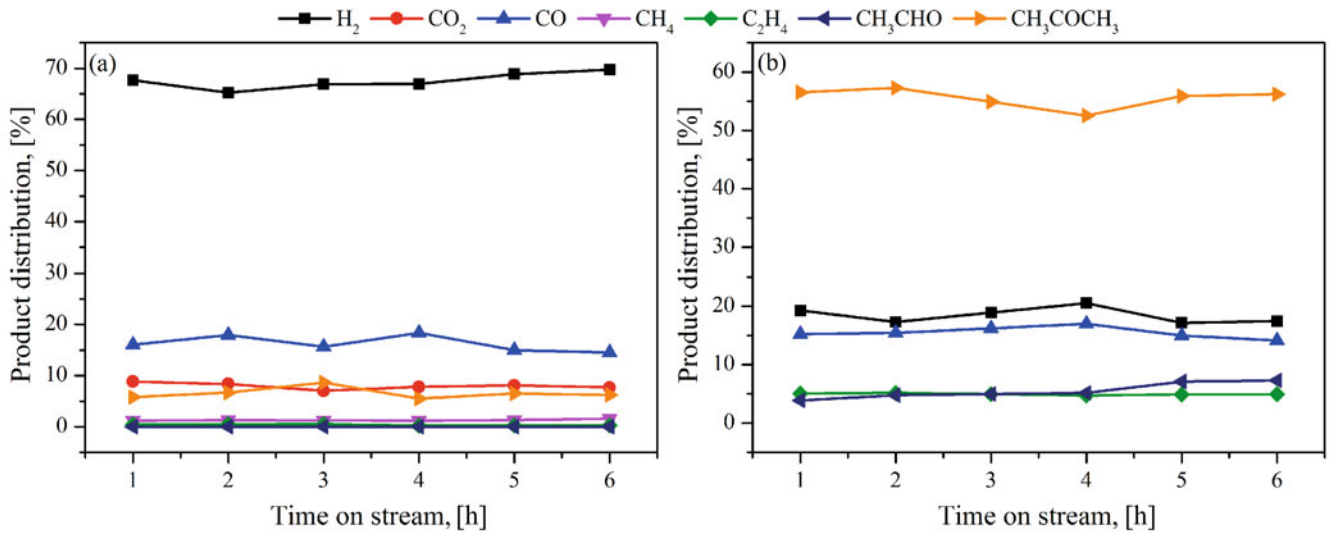

Figure 6. Products distribution as a function of reaction time over 7.5Co,10Ce/HAp catalysts prepared by (a) hydrothermal and (b) sol-gel methods

can be the result of the WGS reaction (during the SRE process decreasing amount of CO in reaction product is observed).

Summarizing, analysis of the SRE results indicates that catalytic behavior of catalysts supported on calcium hydroxyapatite depends strongly on the support synthesis method. The pure hydroxyapatites, independent on the synthesis method, display a slight catalytic performance for the hydrogen production in the SRE process (Table 3) although hydroxyapatite prepared by the hydrothermal route ensures ten times higher hydrogen yield (0.65 mol H_2 per mol C_2H_5OH) than this one synthesized by the sol-gel method (0.06 mol H_2 per mol C_2H_5OH). It can be noted that both supports show a comparable acid-base surface properties (Table 1). However, the textural properties of the HAp supportes are different (Table 1) what may influence on their catalytic performance. The addition of Co and Ce enhances the catalytic properties of the HAp materials. Especially, catalysts supported on HAp-H, i.e. prepared by the hydrothermal method, exhibit a high ethanol conversion and high hydrogen yield as well as favourable products distribution with the highest share of H_2 (Table 3). On the basis of our results and literature data, high activity of Co and Ce containing catalysts can be explained by the coexistence of both Co and Ce centres at various oxidation states together with accompanied oxygen vacancies during the SRE process. XRD pattern of the 5Co,Ce/HAp-H catalyst after SRE process showed that under the reaction conditions, Co_3O_4 was partly reduced to CoO and then to metallic cobalt (Fig. 2). The reduction of Co_3O_4 is the necessary step to achieve the active catalysts for H_2 production because Co_3O_4 is inactive in the SRE process[14]. However, to obtain the high steam reforming activity, the Co^{2+} and Co^0 species should be presented. Studies of cobalt coordination environment under reaction conditions, over supported cobalt catalysts and unsupported Co_3O_4, have been reported by some authors. Over both types of catalysts, Llorca et al.[32–33] observed the coexistence of an equilibrium state between reduced and oxidized phases of cobalt during the SRE process. Moreover, Bayram et al.[14] reported that extent of cobalt reduction is independent of the initial state of the metal on the catalyst surface, and cobalt phase has the same composition under reaction above 450°C. Batista et al.[34] reported that the metallic cobalt sites constituted the active sites for the SRE reaction over cobalt-based catalysts. De la Pena O`Shea et al.[35] observed that while Co_3O_4 was active for dehydrogenation of ethanol leading to acetaldehyde, CoO and Co^0 formed under reaction conditions are the active species in SRE reaction. The catalytic roles of Co^0 and Co^{2+} in SRE pathways were investigated in more detail on Co/MgO catalysts by Karim et al.[36]. The reaction pathways during SRE process were shown to be different on Co^0 and Co^{2+}: Co^0 was much more active than Co^{2+} for ethanol conversion, C-C cleavage and WGS reaction, whereas Co^{2+} enhanced the CH_4 formation. Similar results were obtained by Lebarbier et al.[37], indicating that CoO plays a major role in methane formation. Therefore, it seems that minimization of Co^{2+} species and stabilization of Co^0 against oxidation is crucial to achieve a high H_2 productivity and yield. One should also remember, that the metal-support interactions and the presence of additional metal oxide on the support surface can add another level of complexity for the identification of active species for the steam reforming of ethanol, and the nature and coexistence of the SRE active sites still requires the explanation. We suppose, that modification of HAp supported cobalt catalysts with ceria addition enhances oxygen storage capacity of catalyst system and oxygen mobility, allowing a more effective gasification/oxidation of adsorbed carbon on the catalyst surface. It is in line with literature data, accordingly, Galetti et al.[38] observed that the modification of $Ni/ZnAl_2O_4$ catalysts with CeO_2 inhibits the accumulation of carbon during SRE process depending on the reaction temperature and Ni/Ce ratio whereas Song and Ozkan [39] showed that Co/CeO_2 was more stable under SRE process than cobalt based catalysts supported on other metal oxides due to lower carbon accumulation on its surface. Moreover, CeO_2 is able to interact with metal active component what affects on its redox behavior and can lead to higher dispersion of active cobalt species. It was found by Wang et al.[9] that Co_3O_4/CeO_2 mixed oxides was much more active than either Co_3O_4 or CeO_2 indicating the existence of a synergistic effect between Co_3O_4 and CeO_2. The incorporation of cobalt ions into ceria crystal lattice was beneficial for resistance to carbon deposition. It is also known that the presence of ceria ions favour the water activation-decomposition of water with the subsequent generation of OH groups, which are essential to CO_2 and H_2 formation during SRE process[40].

Results of the TPR-H_2 measurements (Fig. 4, Table 2) show that the Co,Ce/HAp-H catalysts were more reducible (show higher hydrogen consumption) than the Co,Ce/HAp-S catalysts. This suggests that the amount of active sites (Co^0 and Co^{2+}) available for the SRE reaction was higher on these catalysts what ensure the higher hydrogen production. Among the Co,Ce/HAp-H catalysts, the higher hydrogen yield (3.49 mol H_2/mol C_2H_5OH) ensures the catalyst containing 5 wt% Co. With further increase in Co content to 7.5 wt%, the hydrogen yield is decreased. Similar results concerning the effect of cobalt spinel loading was reported by Wang et al.[9].

On the other hand, Co,Ce/HAp-S catalysts also show a high and comparable with the Co,Ce/HAp-H catalysts ethanol conversion (Fig. 5) but do not exhibit the high hydrogen yield and ensure about four times lower H_2 yield than the Co,Ce/HAp-H (Table 3). Moreover, the main product over these catalysts is acetone, whereas share of hydrogen in post reaction effluent is less than 25% (Table 3). For these catalysts, the reduction of Co_3O_4 under reaction conditions seems to be a not sufficient factor to obtain a high level of hydrogen production and suggests that another factors like acid-base and textural properties of materials have a some influence on the catalysts performance. The Co,Ce/HAp-S catalysts are characterized by a two time lower specific surface area than the catalysts supported on the HAp-H, and do not show the significant predominance of basic sites on their surface. It is in line with literature data[16], which indicate that catalysts with acidic surface properties ensure lower catalytic performance in the SRE process. Additionally, these catalysts are the less reducible in comparison to Co,Ce/HAp-H samples (Fig. 4, Table 2). Since CeO_2

can favour the formation of acetone[5] thus we suppose that in the case of Co,Ce/HAp-S catalysts, CeO_2 is the predominantly active phase leading to the increase of acetone amount in reaction products (Fig. 6, Table 3).

Catalytic performances of cobalt catalysts supported on other oxide materials such as CeO_2, La_2O_3, V_2O_5, ZnO, ZrO_2 were already reported for hydrogen production in the SRE process many times. Depending on the reaction conditions and cobalt loading, these catalysts ensured ethanol conversion from 72 to 100%, selectivity toward H_2 from 27 to 93% with hydrogen yield from 2 to 5.5 mol H_2/mol C_2H_5OH[14, 15, 41–42]. The best catalytic performance was obtained for Co/CeO_2 system by Machocki et al[41]. Our studies showed that cobalt and cerium supported on calcium hydroxyapatite could also be the active and efficient catalysts for the steam reforming of ethanol. Further research over catalysts supported on HAp will be conducted for better understanding of the reaction mechanism and the nature of the active SRE sites.

CONCLUSIONS

Studies on cobalt and cerium catalysts supported on the unconventional material, calcium hydroxyapatite, show promising catalytic activity of these systems for hydrogen production via steam reforming of ethanol. As was found, the catalytic performance depends on the preparation method of the support and catalysts. The microwave-assisted hydrothermal and sol-gel methods allow to obtain calcium hydroxyapatites about different properties influencing on catalytic behavior of these materials in SRE process. The cobalt and cerium catalysts supported on hydrothermally prepared HAp exhibited superior performance for hydrogen production. The highest H_2 yield (3.49 mole of hydrogen per mole of ethanol fed), achieved over 5Co,10Ce/HAp–H catalyst, is thought to be due a combination of factors, including increased reducibility and oxygen mobility, higher density of basic sites on its surface, and improved textural properties (higher surface area and porosity).

ACKNOWLEDGMENT

The work was co-financed by a statutory activity subsidy from the Polish Ministry of Science and Higher Education for the Faculty of Chemistry of Wrocław University of Technology (S50068).

LITERATURE CITED

1. Mathure, P.V., Ganguly, S., Patwardhan, A.V. & Saha, R.K. (2007). Steam reforming of ethanol using a commercial nickel-based catalyst. *Ind. Eng. Chem. Res.* 46, 8471–8479. DOI: 10.1021/ie070321k.

2. Soyal-Baltacioglu, F., Aksoylu, A.E. & Önsan, Z.I. (2008). Steam reforming of ethanol over Pt–Ni Catalysts. *Catal. Today* 138, 183–186. DOI: 10.1016/j.cattod.2008.05.035.

3. Basagiannis, A.C., Panagiotopoulou P. & Verykios X.E. (2008). Low temperature steam reforming of ethanol over supported noble metal catalysts. *Top. Catal.* 51, 2–12. DOI: 10.1016/j.cattod.2008.05.035.

4. Erdőhelyi, A., Raskó, J., Kecskés, T., Tóth, M., Dömök, M. & Baán, K. (2006). Hydrogen formation in ethanol reforming on supported noble metal catalysts. *Catal. Today* 116, 367–376. DOI: 10.1016/j.cattod.2006.05.073.

5. Furtado, A.C., Alonso, Ch.G., Cantão, M.P. & Fernandes-Machado, N.R.C. (2009). Bimetallic catalysts performance during ethanol steam reforming: influence of support materials. *Int. J. Hydrogen Energy* 34, 7189–7196. DOI: 10.1016/j.ijhydene.2009.06.060.

6. Lovón, A.S.P., Lovón-Quintana, J.J., Almerindo, G.I., Valenca, G.P., Bernardi, M.I.B., Araújo, V.D., Rodrigues, T.S., Robles-Dutenhefner, P.A. & Fajardo, H.V. (2012). Preparation, structural characterization and catalytic properties of Co/CeO_2 catalysts for the steam reforming of ethanol and hydrogen production. *J. Pow. Sour.* 216, 281–289. DOI: 10.1016/j.jpowsour.2012.05.066.

7. He, L., Berntsen, H. & Chen, D. (2010). Approaching sustainable H_2 production: sorption enhanced steam reforming of ethanol. *J. Phys. Chem. A* 114, 3834–3844. DOI: 10.1021/jp906146y.

8. Haryanto, A., Fernando, S., Murali, N. & Adhikari, S. (2005). Current status of hydrogen production techniques by steam reforming of ethanol: a review. *Energ. Fuel* 19, 2098–2106. DOI: 10.1021/ef0500538.

9. Wang, H., Ye, J.L., Liu, Y., Li, Y.D. & Qin, Y.N. (2007). Steam reforming of ethanol over Co_3O_4/CeO_2 catalysts prepared by different methods. *Catal. Today* 129, 305–312. DOI: 10.1016/j.cattod.2006.10.012.

10. Liberatori, J.W.C., Ribeiro, R.U., Zanchet, D., Noronha, F.B. & Bueno, J.M.C. (2007). Steam reforming of ethanol on supported nickel catalysts. *Appl. Catal. A* 327, 197–204. DOI: 10.1016/j.apcata.2007.05.010.

11. Nishiguchi, T., Matsumoto, T., Kanai, H., Utani, K., Matsumura, Y., Shen, W.J. & Imamura, S. (2005). Catalytic steam reforming of ethanol to produce hydrogen and acetone. *Appl. Catal. A* 279, 273–277. DOI: 10.1016/j.apcata.2004.10.035.

12. Soykal, I.I., Sohn, H. & Ozkan, U.S. (2012). Effect of support particle size in steam reforming of ethanol over Co/CeO2 catalysts. *ASC Catal.* 2, 2335–2348.

13. Llorca, J., Homs, N., Sales, J. & Ramírez de la Piscina, P. (2002). Efficient production of hydrogen over supported cobalt catalysts from ethanol steam reforming. *J. Catal.* 209, 306–317. DOI: 10.1006/jcat.2002.3643.

14. Bayram, B., Soykal, I.I., von Deak, D., Miller, J.T. & Ozkan, U.S. (2011). Ethanol steam reforming over Co-based catalysts: investigation of cobalt coordination environment under reaction conditions. *J. Catal.* 284, 77–89. DOI: 10.1016/j.jcat.2011.09.001.

15. Song, H., Zhang, L. & Ozkan, U.S. (2010). Investigation of the reaction network in ethanol steam reforming over supported cobalt catalysts. *Ind. Eng. Chem. Res.* 49, 8984–8989. DOI: 10.1021/ie100006z.

16. Song, H., Zhang, L. & Ozkan, U.S. (2012) The effect of surface acidic and basic properties on the performance of cobalt-based catalysts for ethanol steam reforming. *Top. Catal.* 55, 1324–1331. DOI: 10.1007/s11244-01209918-8.

17. Park, J.H., Lee, D.W., Im, S.W., Lee, Y.H., Suh, D.J. & Jun, K.W. (2012). Oxidative coupling of methane using non-stoichiometric lead hydroxyapatite catalyst mixtures. *Fuel* 94, 433–439. DOI: 10.1016/j.fuel.2011.08.056.

18. Hakim, L., Yaakob, Z., Ismail, M., Daud, W.R.W. & Sari, R. (2013). Hydrogen production by steam reforming of glycerol over Ni/Ce/Cu hydroxyapatite-supported catalysts. *Chem. Pap.* 67, 703–712. DOI: 10.2478/s11696-013-0368-y

19. Yasukawa, A., Gotoh, K., Tanaka, H. & Kondori, K. (2012). Preparation and structure of calcium hydroxyapatite substituted with light rare earth ions. *Coll. Surf. A.* 393, 53–59. DOI: 10.1016/j.colsurfa2011.10.024.

20. Sugiyama, S., Shono, T., Makino, D., Moriga, T., Hayashi, H. (2003). Enhancement of the catalytic activities in propane oxidation and H-D exchangeability of hydroxyl groups by the incorporation with cobalt into strontium hydroxyapatite. *J. Catal.* 214, 8–14. DOI: 10.1016/S0021-9517(02)00101-X.

21. Aellach, B., Ezzamarty, A., Leglise, J., Lamonier, C. & Lamonier J.F. (2010). Calcium-deficient and stoichiometric hydroxyapatites promoted by cobalt for the catalytic removal of oxygenated volatile organic compounds. *Cat. Lett.* 135, 197–206. DOI: 10.1007/s10562-010-0282-7.

22. Yaakob, Z., Hakim, L., Kumar, M.N.S., Ismail, M., Dau, W.R.W. (2010). Hydroxyapatite supported nickel catalyst for hydrogen production. *Am. J. Sci. Ind. Res.* 1(2) 122–126. DOI: 10.5251/ajsir2010.1.2.122.126.

23. Ogo, S., Onda, A. & Yanagisawa, K. (2008). Hydrothermal synthesis of vanadate-substituted hydroxyapatites, and catalytic properties for conversion of 2-propanol. *Appl. Catal. A* 348, 129–134. DOI: 10.1016/j.apcata.2008.06.035.

24. Jaworski, J.W., Cho, S., Kim, Y., Jung, J.H., Jeon, H. S., Min, B.K. & Kwon, K. (2013). Hydroxyapatite supported cobalt catalysts for hydrogen generation. *J. Coll. Interf. Sci.* 394, 401–408. DOI: 10.1016/j.jcis.2012.11.036.

25. Fathi, M.H. & Hanifi, A. (2009). Sol–gel derived nanostructure hydroxyapatite powder and coating: aging time optimisation. *Adv. Appl. Ceram.* 6, 363–368. DOI: 10.1179/174367609X414080.

26. Martin, D. & Duprez, D. (1997). Evaluation of the acid--base surface properties of several oxides and supported metal catalysts by means of model reactions. *J. Mol. Catal. A-Chem.* 118, 113–128. DOI: 10.1016/S1381-1169(96)00371-8.

27. Konsolakis, M., Sgourakis, M. & Carabineiro, S.A.C. (2015). Surface and redox properties of cobalt-ceria binary oxides: on the effect of Co content and pretreatment conditions. *Appl. Surf. Sci.* 341, 48–54. DOI: 10.1016/j.apsusc.2015.02.188.

28. Liotta, L.F., Di Carlo, G., Pantaleo, G. & Deganello, G. (2005). Co_3O_4/CeO_2 and Co_3O_4/CeO_2-ZrO_2 composite catalysts for methane combustion: correlation between morphology reduction and catalytic activity. *Catal. Commun.* 6, 329–336. DOI: 10.1016/j.catcom.2005.02.006.

29. Liotta, L.F., Ousmane, M., Di Carlo, G., Pantaleo, G., Deganello, G., Boreave, A. & Giroir-Fendler A. (2009). Catalytic removal of toluene over Co_3O_4–CeO_2 mixed oxide catalysts: comparison with Pt/Al_2O_3. Cat. Lett. 127, 270–276. DOI: 10.1007/s10562-008-9640-0.

30. Zanchet, D., Santos, J.B.O., Damyanova, S., Gallo, J. M.R. & Buena, J.M.C. (2015). Toward understanding metal--catalyzed ethanol reforming. *ASC Catal.* 5, 3841–3863. DOI: 10.1021/cs5020755.

31. Batista, M.S., Santos, R.K.S., Assaf, E.M., Assaf, J.M. & Ticianelli, E.A. (2004). High efficiency steam reforming of ethanol by cobalt-based catalysts. *J. Pow. Sour.* 134, 27–32. DOI: 10.1016/j.jpowsour.2004.01.052.

32. Llorca, J., Dalmon, J.A., de la Piscina, P.R. & Homs, N. (2003). In situ magnetic characterization of supported cobalt catalysts under steam-reforming of ethanol. *Appl. Catal. A* 243, 261–269. DOI: 10.1016/S0926-860X(02)00546-X.

33. Llorca, J., de la Piscina, P.R., Dalmon, J.A. & Homs, N. (2004). Transformation of Co_3O_4 during ethanol steam-reforming. Activation process for hydrogen production. *Chem. Mater.* 16, 3573–3578. DOI: 10.1021/cm049311p.

34. Batista, M.S., Santos, R.K.S., Assaf, E.M., Assaf, J.M. & Ticianelli, E.A. (2003). Characterization of the activity and stability of supported cobalt catalysts for the steam reforming of ethanol. *J. Pow. Sour.* 124, 99–103. DOI: 10.1016/S0378-7753(03)00599-8.

35. de la Peña O'Shea, V.A., Homs, N., Pereira, E.B., Nafria, R. & de la Piscina, P.R. (2007). X-ray diffraction study of Co_3O_4 activation under ethanol steam-reforming. *Catal. Today* 126, 148–152. DOI: 10.1016/j.cattod.2006.10.002.

36. Karim, A.M., Su, Y., Engelhard, M.H., King, D.L. & Wang, Y. (2011). Catalytic Roles of Co^0 and Co^{2+} during steam reforming of ethanol on Co/MgO catalysts. *ACS Catal.* 1, 279–286. DOI: 10.1021/cs200014j.

37. Lebarbier, V.M., Karim, A.M., Engelhard, M.H., Wu, Y., Xu, B.Q., Petersen, E.J., Datye, A.K. & Wang, Y. (2011). The effect of zinc addition on the oxidation state of cobalt in Co/ZrO_2 catalysts. *ChemSusChem* 4, 1679–1684. DOI: 10.1002cssc.201100240.

38. Galetti, A.E., Gomez, M.F., Arrúa, L.A. & Abello, M.C. (2008). Hydrogen production by ethanol reforming over NiZnAl catalysts. Influence of Ce addition on carbon deposition. *Appl. Catal. A* 348, 94–102. DOI: 10.1016/j.apcata.2008.06.039.

39. Song, H. & Ozkan, U.S. (2009). Ethanol steam reforming over Co-based catalysts: role of oxygen mobility. *J. Catal.* 261, 66–74. DOI: 10.1016/j.jcat.2008.11.006.

40. Xu, W., Liu, Z., Johnston-Peck, A.C., Senanayake, S.D., Zhou, G., Stacchiola, D., Stach, E.A. & Rodriguez, J.A. (2013). Steam reforming of ethanol on Ni/CeO_2: reaction pathway and interaction between Ni and the CeO_2 support. *ACS Catal.* 3, 975–984. DOI: 10.1021/cs4000969.

41. Machocki, A., Denis, A., Grzegorczyk, W. & Gac, W. (2010). Nano- and micro-powder of zirconia and ceria-supported cobalt catalysts for steam reforming of bio-ethanol. *Appl. Surf. Sci.* 256, 5551–5558. DOI: 10.1016/j.apsusc.2009.12.137.

42. Kumar A., Prasad R. & Sharma Y.C. (2014). Steam reforming of ethanol: production of renewable hydrogen. *Int. J. Environ. Res.* 3, 203–212. From Research India Publication: http://www.ripublication.com/ijerd.htm